PROCEEDINGS OF SCIENCE

^{90,91,92,93,94,96}Zr neutron-capture cross sections from n_TOF

G. Tagliente[1]
I.N.F.N. Bari
Via Orabona, 4 Bari. Italy
E-mail: giuseppe.tagliente@ba.infn.it

M. Lugaro[2], **A.I. Karakas**[3], **P.M. Milazzo**[4] **and n_TOF collaboration**
[2]*Centre for Stellar & Planetary Astrophysics, Monash University, Clayton VIC 3800, Australia,*[3]*Research School of Astronomy & Astrophysics, Mount Stromlo Observatory, Weston Creek ACT 2611, Australia,* [4] *Istituto Nazionale di Fisica Nucleare (INFN), Trieste, Italy*

Based on the characteristic features of the n_TOF facility at CERN, accurate measurements of the (n, γ) cross sections have been performed for all stable Zr isotopes as well as for the radioactive isotope ^{93}Zr, providing a new set of cross sections that can be used in stellar models..

The Zr neutron-capture cross sections from the n_TOF experiment have been included in models of the *slow* neutron-capture process (the s process) in C-rich Asymptotic Giant Branch stars; the model results have been compared to data from single mainstream silicon carbide and high-density graphite grains extracted from meteorites. The new cross sections result in an overall better match between the models and the observational data. We also discuss the perspective for new measurements.

XII International Symposium on Nuclei in the Cosmos

[1] Speaker

PoS(NIC XII)025

PROCEEDINGS OF SCIENCE

August 5-12, 2012
Cairns, Australia

PoS(NIC XII)025

1. Introduction

Accurate s-process analyses have attracted great interest over the last decade, thanks to the progresses in astronomical observation and in stellar modeling. The understanding of the s process has advanced from a phenomenological description of the abundance distribution in the solar system towards a comprehensive picture, which includes the overall aspects of stellar and galactic evolution [1]. In particular, this development has shown the importance of neutron-capture nucleosynthesis for probing the evolution of Asymptotic Giant Branch (AGB) stars. The success of the stellar s-process models could be achieved also due to the significant improvements in the neutron capture cross section data, which reached uncertainties of only a few %. At present, however, many cross section data are still missing, particularly in the mass region A≤100 as well as for neutron magic nuclei where cross sections are small and dominated by isolated resonances [2]. The Zr isotopes represent an important example of this situation. Situated at and near magic neutron number N = 50, the Zr isotopes take a particular position on the s-process path, at the border between the *weak* and *main* component, which dominate the s-abundances between Fe and Sr and from Sr up to the Pb/Bi region, respectively. The weak component takes place in massive stars during the convective core He-burning and shell C-burning phases of the pre-supernova evlotution [3], while the main component occurs in AGB stars of masses between roughly $1 \leq M/M_{\odot} \leq 3$ (where $M_{\odot}$ denotes the mass of the Sun). Because of their magic or near magic neutron configurations all Zr isotopes exhibit relatively small (n,γ) cross sections and, in turn, comparably high s abundances. This holds especially for the neutron magic nucleus ^{90}Zr, but also for the stable isotopes ^{91}Zr, ^{92}Zr, and ^{94}Zr, which are all predominantly of s-process origin.

As far as the unstable isotopes ^{93}Zr and ^{95}Zr are concerned, the first can be considered as stable on the time scale of the s process because of its long half-life of 1.5 Myr. The s-abundance of ^{93}Zr decays only later to provide the s-component of the daughter ^{93}Nb, which lies outside the main s-process path. The second, ^{95}Zr represents a branching point on the s-process path, where the reaction flow splits due to the competition between (n,γ) reactions and β decays. The relatively short half-life of ^{95}Zr ($t_{1/2}$= 64 d) prevents a large part of the reaction flow from reaching ^{96}Zr. Therefore, ^{96}Zr is traditionally considered as a r process product with a small s process admixture [1, 4], given that it may be fed by the s process only at neutron densities in excess of 3×10^{8} cm^{-3}. To some extent, the s-production of ^{96}Zr is favored, however, by its low neutron capture cross section, which plays a key role in the analysis of the branching at A = 95.

In general, s-process branchings represent unique possibilities for constraining the physical conditions in the He-burning zone of the AGB stars locate just above the C-O degenerate core [5, 6, 7]. The ^{95}Zr branching is sensitive to the conditions prevailing in AGB stars, where ^{96}Zr is depleted between He-shell flashes, as a result of the low neutron density produced by the ^{13}C neutron source, and replenished during the He-shell flashes, as a result of the high neutron densities produced by ^{22}Ne(α, n) reactions. Thus, the s-abundance of ^{96}Zr can be interpreted as an indicator for the efficiency of the ^{22}Ne neutron source.

Important constraints on stellar nucleosynthesis can be obtained by the study of circumstellar dust grains recovered from meteorites [8]. In fact, the isotopic pattern of Zr observed in presolar grains [9] and particularly the relative abundances of ^{94}Zr and ^{96}Zr in silicon carbide (SiC) grains, which originate from AGB stars, provide information on the s-process efficiency in the parent stars.

2. n_TOF facility at CERN

Based on an idea by Rubbia et al. [10], the n_TOF facility at CERN (Geneva, Switzerland) became fully operational in May 2002 [11]. After commissioning of the neutron beam, an intense scientific program has started, relevant for Nuclear Astrophysics and Nuclear Energy applications. At n_TOF, neutrons are produced via spallation reactions induced by a pulsed proton beam on a massive lead target of 80 x 80 x 60 cm^3. The high proton momentum of 20 GeV/c, the short pulse width of 6 ns, and an intensity of $7 \cdot 10^{12}$ protons per pulse make n_TOF one of the most luminous neutron source worldwide. A 5.8 cm water slab surrounds the lead target acting as a coolant and as moderator of the initial fast neutron spectrum. As a result, a white neutron spectrum ranging from thermal up to a few GeV is produced [12].

Neutrons emerging from the target propagate in the vacuum pipe inside a time-of-flight tunnel 200 m long. Two collimators are present along the flight path: one with a diameter of 13.5 cm placed at 135 m from the lead target, and one at 180 m with a diameter of 2 cm for the capture measurements. This collimation results in a Gaussian-shaped beam profile [13]. A 1.5 T sweeping magnet placed at 40 m upstream of the experimental area is used to deflect outside the beam charged particles travelling along the vacuum pipe. For an efficient background suppression, several concrete and iron walls are placed along the time-of-flight tunnel.

The measuring station is located inside the tunnel, centered at 187.5 m from the spallation target.

Two complementary setups for neutron capture measurement are used at n_TOF: a pair of specifically designed C_6D_6 [14], and a 4π BaF_2 array [15] acting as a total absorption calorimeter (TAC). Due to the low neutron capture cross-section of the Zr isotopes the C_6D_6 detectors were preferred for these measurements, since these detectors have the advantage of presenting an extremely low sensitivity to scattered neutrons.

The data acquisition system is based on flash ADCs with sampling rate up to 1 GHz. The consequent very high data rate ensures an almost zero dead time [16].

2.1 Samples

The characteristic of the samples are summarized in Table 1. The enriched Zr samples were prepared from oxide powder; all the samples were encapsulated in Al container. Due to its natural radioactivity, 62.6 MBq, the ^{93}Zr sample was also encapsulated in a Ti container. An admixture of Hf, Na, Mg, Al, Sn and Mo were also present in the Zr samples. The influence of those contaminants, although small (their total contamination was lower than 1%), can not be neglected. An additional Au reference sample, as well as a natural C and ^{208}Pb samples, were used for neutron flux normalization in the measurements. The Au reference sample was used

because the gold capture cross section is known with high accuracy, particularly the saturated resonance at 4.9 eV. The C and ^{208}Pb samples were used to determine the background components related to sample scattered neutrons and in-beam γ rays.

Table 1: Characteristics of the Zr samples used in the measurements

Isotope	Diameter (mm)	Mass (g)	Enrichment(%)
^{90}Zr	22	2.721	97.7
^{91}Zr	22	1.407	89.9
^{92}Zr	22	1.351	91.4
^{93}Zr	22	4.46	19.98
^{94}Zr	22	2.015	91.4
^{96}Zr	22	3.401	58.5

3. Determination of the capture yields

Neutron capture reactions are characterized by the prompt γ-ray cascade emitted from the compound nucleus. In order to detect capture events independently of the cascade multiplicity, the intrinsic efficiency of C_6D_6 detectors has to be corrected by the pulse height weighting technique (PHWT) [17–19]. The PHWT represents an *a posteriori* manipulation of the detector response to ensure that the detector efficiency increases linearly with γ-ray energy. Then, the efficiency for capture cascades becomes proportional to the total released γ energy. To obtain the required linearity with γ-ray energy, each detector signal is multiplied with a weighting function (WF), a parameterized polynomial function of Eγ. Provided that the weighting function is properly determined, it has been demonstrated by a detailed study of the possible systematic uncertainties that an accuracy of 2% can be achieved with the PHWT [19].

Given the low neutron capture cross section of the Zr isotopes, the characterization of all possible backgrounds is of primary importance for these measurements. Different background components were identified: (i) capture of sample-scattered neutrons in the detectors or in surrounding materials, (ii) capture events in the aluminum can of the Zr sample, (iii) the ambient background in the experimental area, and mainly (iv) in-beam γ rays produced in the spallation target. The evaluation of these backgrounds has been discussed in detail elsewhere [20].

Finally, the measured yield has been normalized by means of the saturated resonance technique [21], using the 4.9 eV resonance of ^{197}Au in the TOF spectrum of the 0.1-mm-thick Au sample. This absolute yield is directly linked to the capture and total cross sections and has been subject to an R-matrix analysis, using the SAMMY code in the Reich-Moore approximation [22], to extract the individual resonance parameters. The resonance parameters for all the isotopes measured are reported in [23-28].

4. Maxwellian Averaged Cross Sections

The Maxwellian-averaged capture cross sections (MACS), which are required for the

quantitative description of the s-abundances produced by the weak and main component [26], have been calculated by folding the capture cross section with the thermalized stellar spectra over a sufficiently wide neutron energy range, starting at about 100 eV and extending to about 500 keV, the highest temperatures reached during shell carbon burning in massive stars.

In any case, the contribution from massive stars to the Zr isotopes is limited to about 2% [3, 29, 30]; therefore, the improved MACS of the Zr isotopes have negligible consequences on the abundance of Zr isotopes provided by the weak component, while they impact predominantly on the s-component produced in AGB stars.

In Table 2 are reported the MACS values determined for three typical s process situations: for the stellar environments in thermally-pulsing low-mass AGB stars where neutrons are released by (α, n) reactions on ^{13}C and ^{22}Ne, KT = 8 and 23 keV, respectively. The values for ^{95}Zr are obtained normalizing the systematic of the MACS of the even isotopes to the experimental values for the odd isotopes [31].

Table 2 MACS determined for two typical s-process termperatures [22-27]

Isotope	KT = 8 keV	23 keV
^{90}Zr	38 ± 4	22 ± 2
^{91}Zr	170 ± 10	77 ± 5
^{92}Zr	97 ± 5	44 ± 3
^{93}Zr	252 ± 12	117 ± 10
^{94}Zr	58 ± 3	34 ± 2
^{95}Zr	89.1	26.3
^{96}Zr	33 ± 1	11 ± 0.6

5. Implications on the comparison of the AGB models to the composition of the stardust grains

To model the nucleosynthesis in AGB stars the Monash-Mt Stromlo stellar structure code [32,33] has been used. The detailed s-process nucleosynthesis was calculated using a post-processing code that takes information on the stellar structure, such as temperature, densities, and convective velocities, and solves implicitly the set of equations that describes simultaneously changes of the stellar abundances due to the mixing and to nuclear reaction. This method is described in more detail in [34].

Figure 1 presents the values obtained for three selected Zr isotopic ratios at the stellar surface of four computed stellar AGB models using the Zr neutron-capture cross sections from this work and from Ref. [2]. These are compared to the Zr composition measured in single stardust SiC and high-density graphite grains. Using the new MACs the match between the models and the grains improves for the ^{90}Zr/^{94}Zr and ^{96}Zr/^{94}Zr ratios, while it is slightly worse in the case of the ^{92}Zr/^{94}Zr ratio. For the ^{91}Zr/^{94}Zr ratio, not shown in the figure, there is no substantial change and the stardust data are generally well matched (see also Ref. [9]). In the models presented in Fig.1 the extent in mass of the proton profile assumed to penetrate from the convective envelope in the He intershell at the end of each third dredge-up episode is set to

0.002 $M_{\odot}$, and the number of protons is set to decrease exponentially with the mass. The protons are captured by the ^{12}C producing ^{13}C "pocket" were most of the neutrons are released in low-mass AGB models. When we reduce the extent in mass of the proton profile obviously a lower abundance of ^{13}C results, lower s-process abundances are produced and the Zr isotopic ratios at the stellar surface shift towards the solar composition at δ=0, providing an opportunity to match more of the grain data. These models will be presented and discussed in mode details in a forthcoming paper.

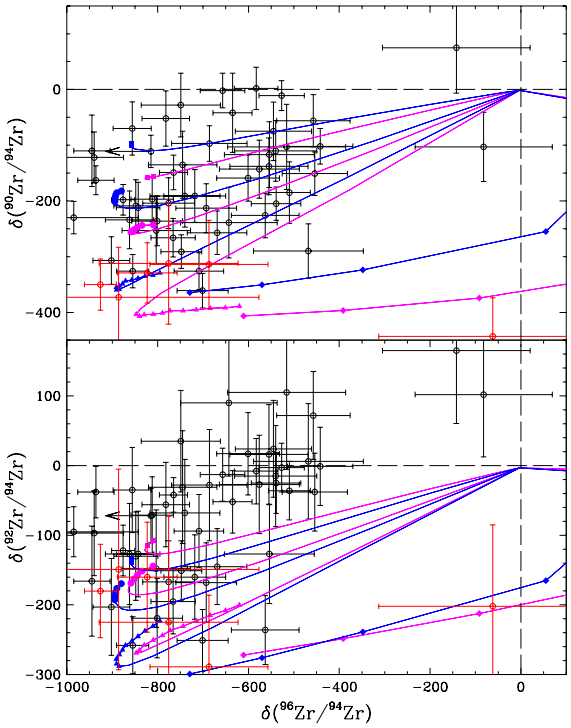

Figure 1 Comparison between AGB models computed with different Zr neutron-capture cross sections and the composition of sturdust grains for three selected Zr isotopic ratios. The δ notation represent permil variations with respect to the solar ratios at δ=0 (e.g. δ=50 is 5% higher than solar). The symbols with associated 2σ error bars represent data for SiC grains (black) and high-density graphite (red). The lines represent the evolution of the isotopic ratios at the surface of four different AGB model, where full symbols are used when C > 0 at the stellar surface. ● $3M_{\odot}$ Z=0.02, ▲ $3M_{\odot}$ Z=0.01, ■ $3M_{\odot}$ Z=0.03, ◆ 1.8 $M_{\odot}$ Z=0.01. Different choices of the Zr neutron-capture cross section are represented by symbols of different colour: magenta symbols Ref. [2]; blue symbols this work.

6. Conclusions and perspectives

The (n,γ) cross sections of ^{90,91,92,93,94,96}Zr have been measured with improved accuracy taking advantage of the unique features of the n TOF facility at CERN. Resonance parameters, the capture kernels, and the MACSs were determined. The MACSs of the Zr isotopes measured were found to be different than reported in previous TOF measurements. This might be the consequence of improvements concerning the experimental setup and the data analysis package.

The new cross sections result in an overall better match between the models and the stardust data, particularly for the ^{96}Zr/^{94}Zr and ^{90}Zr/^{94}Zr ratios, but some of the measured ^{92}Zr/^{94}Zr ratios are still ~10% higher than predicted.

Although the neutron-capture cross section measured were made in a wide range of energies, the data still needed to be complemented by evaluated data from the libraries**.** To allow the most accurate possible calculation of the MACs new measurements are needed both to confirm the results obtained so far and to extend the neutron energy investigated.

The n_TOF facility was recently upgraded to allow measurements of unsealed radioactive samples. Furthermore, thanks to a new moderator and cooling system, the background has now been reduced by more than a factor of 10. These new features of the n_TOF facility may now allow to extend the measurement of these important reactions to a wider energy region. In 2012 new measurements of ^{92,93}Zr isotopes have been performed, the new results are expected to improve the accuracy of the MACS for these isotopes.

References

[1] F. Käppeler, Prog. Nucl. Part. Phys. 43, 419(1999).

[2] Z. Bao et al., Atomic Data Nucl. Data Table 76, 70(2000).

[3] C.M. Raiteri, R. Gallino, M. Busso, D. Neuberger, and F. Käppeler, Ap. J., 419(1993)207.

[4] A.G.W. Cameron, Space Sci. Rev. 15, 121(1973).

[5] R. Gallino, C. Arlandini, M. Busso, M. Lugaro, C. Travaglio, O. Straniero, A. Chieffi, and M. Limongi, Ap. J. 497, 388(1998).

[6] C. Arlandini, F. Käppeler, K. Wisshak, R. Gallino, M. Lugaro, M. Busso, and O. Straniero, Ap. J. 525, 886(1999)

[7] M. Lugaro, F. Herwig, J.C. Lattanzio, R. Gallino, and O. Straniero, Ap. J. 586, 1305(2003).

[8] E. Anders and E. Zinner, Meteoritics 28, 490(1993).

[9] M. Lugaro, A.M. Davis, R. Gallino, J. Pellin, O. Straniero, and F. Käppeler, Ap. J. 593, 486(2003).

[10] C. Rubbia et al. *A high Resolution Spalation driven Facility at the CERN-PS to measure Neutron Cross Sections in the Interval from 1 eV to 250 MeV*. CERN/LHC/98-02 (EET)- Add.1. CERN. Geneva. 1998.

[11] *Proposal for a Neutron Time of flight Facility*, CERN-SPSC 99-8, SPSC/P 310, 17 March 1999

[12]

[13] U. Abbondanno et al. , Tech. Rep. CERN/SL/2002-053 ECT(2003).

[14] *S. J. Pancin et al.* , Nucl. Instr. Meth. A 524 (2004)102.

[15] R. Plag et al. , Nucl. Instr. Meth. A 496 (2003)425.

[16] C. Guerrero et al., Nucl. Instr. Meth. A 608 (2009)424

[17] U. Abbondanno et al., Nucl. Instr. and Meth. A 538 (2005)692.

[18] F. Corvi *et al.*, Nucl. Sci. Eng. **107**, 272 (1991).

[19] J. N. Wilson *et al.*, Nucl. Instrum. Methods A **511** (2003)388.

[20] U. Abbondanno *et al.*, Nucl. Instrum. Methods A **521** (2004)454.

[21] R. L. Macklin and J. Halperin, Phys. Rev. C **14**, 1389(1976).

[22] N. M. Larson, *Updated Users' Guide for SAMMY: Multilevel R-matrix fits to neutron data using Bayes' equations, SAMMY computer code*, Report No. ORNL/TM-9179/R7, Oak Ridge National Laboratory, 2006.

[23] G.Tagliente et al., Phys. Rev. C 77, 035802(2008)

[24] G.Tagliente et al., Phys. Rev. C 78, 045804(2009)

[25] G.Tagliente et al., Phys. Rev. C 81, 055801(2010)

[26] G.Tagliente et al., Phys. Rev. C 84, 015801(2011)

[27] G.Tagliente et al., Phys. Rev. C 84, 055802(2011)

[28] G.Tagliente et al., Phys. Rev. C 87, 014622(2013)

[29] S.P. Kapchigashev, and Yu.P. Popov. Soviet Journal of Nuclear Physics. 4 (1967) 486.

[30] K.A. Toukan and F. Käppeler. Ap. J. 348(1990) 357.

[31] K. Shibata et al. J. Nucl. Sci. Technol. 39 (2002) 1125.

[32] Lattanzio, J., Frost, C., Cannon, R., & Wood, P. Mem. Soc. Astron., 67(1996) 729.

[33] Karakas, A. I., Lattanzio, J. C., & Pols, O. R. Publ. Astron. Soc. Australia,19(2002) 515.

[34] M. Lugaro, C. Ugalde, A. I. Karakas, J. Görres, M. Wiesher, J. C. Lattanzio & R. C. Cannon. Ap. J. 615(2004) 934.